arXiv:1210.1398v1 [cond-mat.str-el] 4 Oct 2012

Charge and Spin Fractionalization Beyond the Luttinger Liquid Paradigm

Alexander Moreno,[1] Alejandro Muramatsu,[1, 2] and José M. P. Carmelo[1, 2, 3]
[1]*Institut für Theoretische Physik III, Universität Stuttgart,*
Pfaffenwaldring 57, D-70550 Stuttgart, Germany
[2]*Beijing Computational Science Research Center, Beijing, 100084, China*
[3]*Center of Physics, University of Minho, Campus Gualtar, P-4710-057 Braga, Portugal*
(Dated: October 5, 2012)

It is well established that at low energies one-dimensional (1D) fermionic systems are described by the Luttinger liquid (LL) theory, that predicts phenomena like spin-charge separation, and charge fractionalization into chiral modes. Here we show through the time evolution of an electron injected into a 1D t-J model, obtained with time-dependent density matrix renormalization group, that a further fractionalization of both charge and spin takes place beyond the hydrodynamic limit. Its dynamics can be understood at the supersymmetric point ($J = 2t$) in terms of the excitations of the Bethe-Ansatz solution. Furthermore we show that fractionalization with similar characteristics extends to the whole region corresponding to a repulsive LL.

PACS numbers: 05.30.Fk, 71.10.Fd, 71.10.Pm

There is a sustained interest in the physics of one-dimensional (1D) quantum systems due to recent experimental advances that allow to access exotic phenomena like spin-charge separation and charge fractionalization [1]. At low energies these systems are well described by the Luttinger Liquid (LL) theory [2] that predicts two independent excitations carrying either only charge (holons) or only spin (spinons) and propagating with different velocities, and hence, spin-charge separation. Experimental evidences of its existence have been observed in quasi-1D organic conductors [3], semiconductor quantum wires [4], and quantum chains on semiconductor surfaces [5]. The LL theory also predicts the fractionalization of injected charge into two chiral modes (left- and right-going) [6], a phenomenon recently confirmed experimentally [7]. Along the experimental advances also theoretical progress was recently achieved pertaining extensions beyond the LL limit by incorporating nonlinearity of the dispersion, leading to qualitative changes in the spectral function [8–12] and relaxation processes of 1D electronic systems [13].

Here we show that fractionalization of charge and spin beyond the forms described by LL theory takes place when a spin-1/2 fermion is injected into a strongly correlated 1D system, namely the t-J model. By studying the time evolution of the injected wavepacket at different wavevectors k, using time-dependent density matrix renormalization group (t-DMRG) [14–19] different regimes were obtained. When k is close to the Fermi wavevector k_F, the known features from LL theory like spin-charge separation and fractionalization of charge into two chiral modes result. On increasing k, a further fractionalization of charge and spin appears, in forms that depend on the strength of the exchange interaction J or the density n. Their dynamics can be understood at the supersymmetric (SUSY) point $J = 2t$ in terms of charge and spin excitations of the Bethe-Ansatz solution [20–22]. For the region of the phase diagram [23, 24], where the ground state corresponds to a repulsive LL, two qualitatively different regimes are identified: one regime with $v_s > v_c$ and another where $v_s < v_c$. Here $v_{c(s)}$ is the velocity of the excitations mainly carrying charge (spin). For $v_s > v_c$ and $k > k_F$ the spin excitation starts to carry a fraction of charge that increases with k while v_c corresponds to a wavepacket carrying only charge. For $v_s < v_c$ and $k > k_F$ the situation is reversed and the fastest charge excitation carries a fraction of spin that increases with k while the wavepacket with v_s carries almost no charge, i.e. in this case spin fractionalizes.

The Hamiltonian of the 1D t-J model is as follows,

$$H = -t \sum_{i,\sigma} \left(\tilde{c}^{\dagger}_{i,\sigma} \tilde{c}_{i+1,\sigma} + \text{h.c.} \right) + J \sum_{i} \left(\vec{S}_i \cdot \vec{S}_{i+1} - \frac{1}{4} n_i n_{i+1} \right), \tag{1}$$

where the operator $\tilde{c}^{\dagger}_{i,\sigma}$ ($\tilde{c}_{i,\sigma}$) creates (annihilates) a fermion with spin $\sigma = \uparrow, \downarrow$ on the site i. They are not canonical fermionic operators since they act on a restricted Hilbert space without double occupancy. $\vec{S}_i = \tilde{c}^{\dagger}_{i,\alpha} \vec{\sigma}_{\alpha\beta} \tilde{c}_{i,\beta}$ is the spin operator and $n_i = \tilde{c}^{\dagger}_{i,\sigma} \tilde{c}_{i,\sigma}$ is the density operator.

We study the time evolution of a wavepacket, corresponding to a fermion with spin up injected into the ground state, by means of t-DMRG [14–19]. The state of a gaussian wavepacket $|\psi\rangle$ centered at x_0, with width Δ_x and average momentum k_0, is created by the operator $\psi^{\dagger}_{\uparrow}$ applied onto the ground state $|G\rangle$:

$$|\psi\rangle \equiv \psi^{\dagger}_{\uparrow} |G\rangle = \sum_i \varphi_i \tilde{c}^{\dagger}_{i\uparrow} |G\rangle, \tag{2}$$

with

$$\varphi_i = A e^{-(x_i - x_0)^2 / 2\Delta_x} e^{i k_0 x_i}. \tag{3}$$

A is fixed by normalization. The time evolved state $|\psi(\tau)\rangle$ by the Hamiltonian (1) determines the spin (s) and charge (c) density relative to the ground state as a function of time τ measured in units of $1/t$ ($\hbar = 1$),

$$\rho_\alpha(x_i, \tau) \equiv \langle\psi(\tau)|n_{i\alpha}|\psi(\tau)\rangle - \langle G|n_{i\alpha}|G\rangle, \qquad (4)$$

where $\alpha = s, c$, $n_{ic} = n_{i\uparrow} + n_{i\downarrow}$, and $n_{is} = n_{i\uparrow} - n_{i\downarrow}$. Most of the numerical results were carried out on systems with $L = 160$ lattice sites, using 600 DMRG vectors (this translates into errors of the order of 10^{-4} in the spin and charge density up to times of $50/t$) and $\Delta_x = 5$ lattice sites (which corresponds to a width $\Delta_k \sim 0.06\pi$ in momentum space).

We discuss first the time evolution of a wavepacket at the SUSY point $J = 2t$, since here we will be able to identify the different portions in which the wavepacket splits on the basis of the Bethe-Ansatz solution. Figure 1 shows the time evolution of $\rho_c(x_i, \tau)$ for a density of $n = 0.6$ ($n \equiv N/L$, with N the number of fermions). The momentum of the injected fermion is $k = 0.7\pi$, i.e. midway between $k_F = 0.3\pi$ and the zone boundary. The charge (i.e. ρ_c) splits into four fractions, one portion traveling to the left and the rest doing so to the right. A splitting into chiral modes is expected in the frame of LL theory [6], where for an injected right-going fermion, a splitting $Q_\alpha^{(\pm)} = (1 \pm K_\alpha)/2$ (where K_α is the so-called LL parameter and '+' ('-') corresponds to the right (left) propagating part) is predicted. The amount of charge (i.e. the integral of the wavepacket over its extension) corresponding to the portion denoted P_1 is $Q_c^{(-)} \sim 0.1$ which agrees well with the prediction of LL theory, since for the parameters in this case, $K_c \sim 0.8$ [24]. However, at long enough times, a further splitting of the right-going charge is observed (wavepackets P_i with $i = 2, 3, 4$), beyond the prediction of the LL theory.

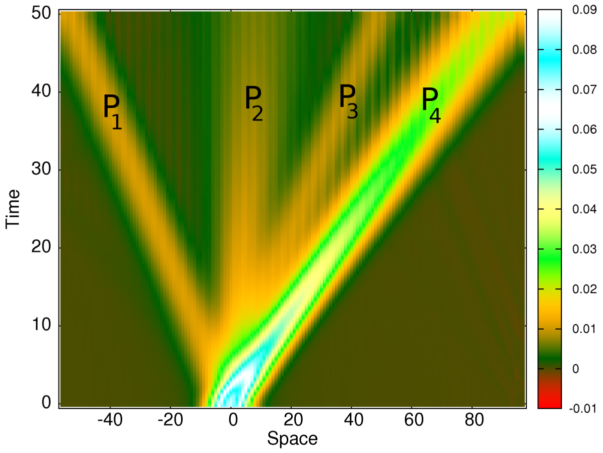

FIG. 1. (color online). Time evolution of $\rho_c(x_i, \tau)$ for a wavepacket initially at $x = 0$, with momentum $k = 0.7\pi$, at density $n = 0.6$, and $J = 2t$. Charge fractionalizes into four wavepackets, one to the left(P_1) and the rest(P_2, P_3, P_4) to the right. P_1 and P_3 have the same charge and speed but opposite velocities.

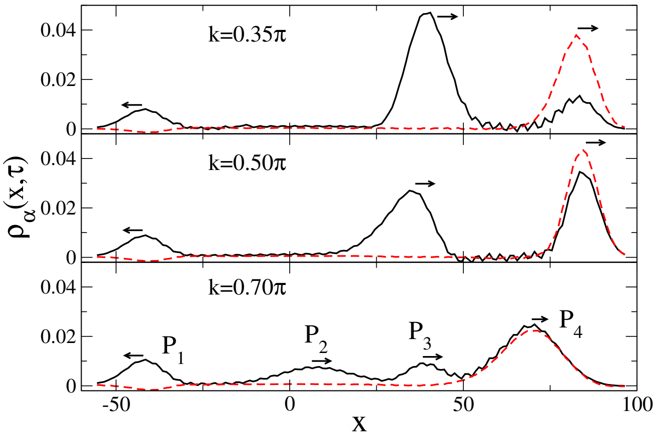

FIG. 2. (color online). Charge ($\rho_c(x_i, \tau)$, full line) and spin ($\rho_s(x_i, \tau)$, dashed line) densities for $J = 2t$, $n = 0.6$, at time $\tau = 40$, for different values of the momentum of the injected fermion.

Figure 2 displays both $\rho_c(x_i, \tau)$ (full line) and $\rho_s(x_i, \tau)$ (dashed line) for different values of the initial momentum of the injected wavepacket. The arrows indicate the direction of motion of each packet. As opposed to ρ_c, ρ_s does not split. In an SU(2) invariant system $K_s = 1$ [2], and hence $Q_s^{(-)} = 0$, i.e. no left propagating part is expected for the spin density. (However, a small depletion in ρ_s appears traveling to the left, which would correspond to $K_s \gtrsim 1$. Similar findings were presented recently [25] and attributed to finite-size effects that require exponentially large systems in order to recover $K_s = 1$.) Moreover, part of the charge (P_4) is accompanying the spin, such that spin-charge separation does not appear to be complete. The amount of charge accompanying the spin increases as the momentum of the injected fermion approaches the zone boundary. These results make already evident that injecting a fermion at a finite distance from the Fermi energy leads to fractionalization of charge beyond the expectations from the LL theory.

In order to understand the new forms of fractionalization that go beyond the LL frame, we consider the excitations corresponding to one-particle addition processes, whose energies can be obtained from the Bethe-Ansatz solution [12, 26]. When adding an electron with momentum k, the single particle excitation energy is given by $\omega(k) = -\epsilon_c(q_c) - \epsilon_s(q_s)$, where $\epsilon_c(q_c)$ and $\epsilon_s(q_s)$ are the dispersion relations of the excitations for charge and spin, respectively, and the momenta are related to the momentum of the incoming particle as follows: $k = \pm 2k_F - q_c - q_s$, where $q_c \in [-q_{Fc}, q_{Fc}]$, and $q_s \in [-q_{Fs}, q_{Fs}]$, with $q_{Fc} = \pi - 2k_F$ and $q_{Fs} = \pi - k_F$ the pseudo-Fermi momenta for the excitations for charge and spin, respectively [22, 27].

Figure 3 displays the velocities obtained from t-DMRG

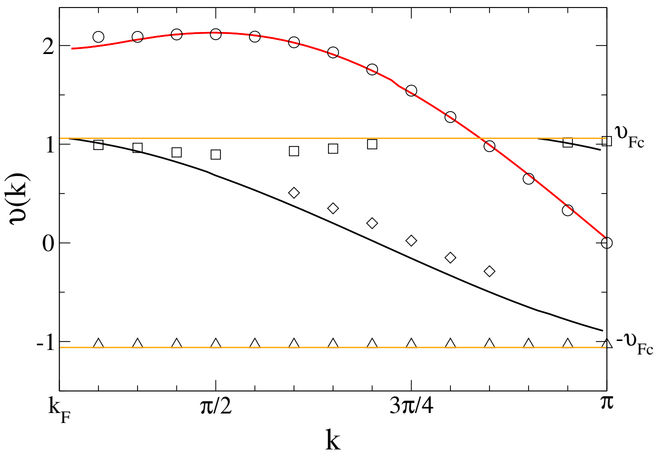

FIG. 3. (color online). Full lines: derivatives $v_\alpha(k) = \partial\epsilon_\alpha(k)/\partial k$ of the dispersions obtained by the Bethe-Ansatz solution. The symbols correspond to the velocities of the different wavepackets identified in Fig. 2: triangles(P_1), diamonds(P_2), squares(P_3) and circles(P_4). The orange horizontal lines stand for the Fermi velocity $v_{Fc} = \partial\epsilon_c(q_{Fc})/\partial q$ given by the Bethe-Ansatz solution.

for the different wavepackets (symbols) compared to those obtained from Bethe-Ansatz (full lines), as a function of the momentum of the injected fermion. The velocity of each P_i is extracted by measuring the position of the maximum of the packet at the most convenient time, i.e, at that time where we can resolve P_i and the spreading of one packet does not destroy the other packets. The wavepackets P_1 (triangles) and P_3 (squares) have opposite directions, but the same speed and charges $Q_c^{(-)} \simeq Q_{c3}^{(+)}$, where the charges for the (+) branch are labelled by an index corresponding to the respective wavepackets. The velocity of the wavepacket P_4 (circles) agrees almost perfectly with the one corresponding to spin excitations. Its determination is best since it is the fastest wavepacket, such that it can be easily discerned from the rest. The velocity of the remaining wavepacket, P_2 (diamonds), is more difficult to assess, since it overlaps at the beginning with other ones. Nevertheless, its velocity closely follows the one of charge excitations. The wavepackets just described deliver a direct visualization of the excitations appearing in the Bethe-Ansatz solution, where only two different kind of particles are involved: the c and s pseudoparticles with their associated bands. The excitation associated with spin involves one hole in the c band with fixed momentum q_{Fc} and one hole in the s band with momentum q_s, where $q_s = \pm 2k_F - q_{Fc} - k$ [22]. In fact, the velocities of P_1 and P_3 correspond to the group velocity at both pseudo-Fermi momenta $\pm q_{Fc}$. Furthermore, as shown in Fig. 3, the velocity of those fractions is independent of the momentum of the injected fermion, in agreement with the picture given by Bethe-Ansatz. The dispersion of the hole in the s-band gives rise to the velocity displayed by the red line in Fig. 3. Similarly, the c line (black line in Fig. 3) involves one hole in the s band with fixed momentum q_{Fs} and one hole in the c band with momentum q_c determined in terms of k by $q_c = \pm 2k_F - q_{Fs} - k$. Using the same argument as for the s line we can associate the P_2 packet (diamonds) with the c pseudoparticle. However, in this case we cannot observe wavepackets associated with spin and velocities corresponding to the group velocity at the pseudo-Fermi momenta $\pm q_{Fs}$. We understand this as due to the fact that $K_s = 1$, by analogy to what we observe in the $K_c = 1$ case. On the SUSY point this case is reached in the limit of vanishing density, where the system can be described by a Fermi gas. Hence, fractionalization is absent in this limit.

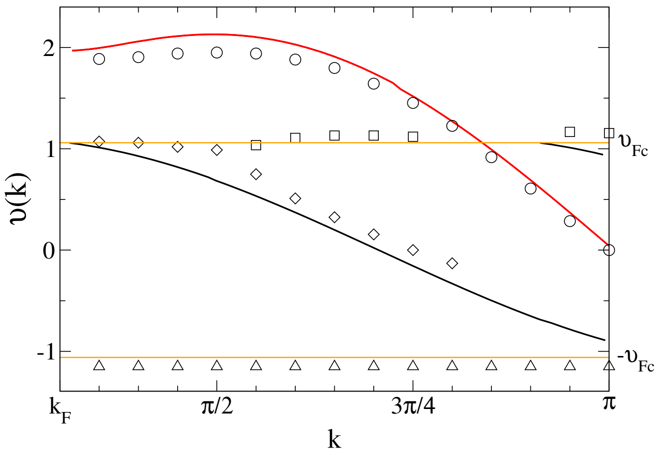

FIG. 4. (color online). As in Fig. 3 but for $J = 1.75t$. The fullines correspond to the SUSY Bethe ansatz.

Next we depart from the SUSY point and examine how fractionalization takes place in the region of the phase diagram where the ground state corresponds to a LL with $K_c < 1$. Figure 4 shows the velocity of the different fractions at $J = 1.75t$, where a slight decrease (increase) in the velocity of the spin (density) fraction can be observed. As shown in Fig. 5, essentially the same features are observed as at the SUSY point both for $J > 2t$ and $J < 2t$. In all the cases shown in Fig. 5, where the velocity of spin excitations (v_s) remains higher than that of charge excitations (v_c) in most parts of the Brillouin zone, spin does not fractionalize, as opposed to charge, so that the interpretation derived from Bethe-Ansatz remains valid over an extended region of the phase diagram: charge splits into four portions of which one travels with the spin wavepacket, and two have the same speed but opposite group velocity which does not depend on the momentum of the injected fermion. It is tempting to assign those excitations to states at a pseudo-Fermi surface for charge excitations.

For smaller values of J/t than those in Fig. 5, v_s becomes smaller than v_c. Figure 6 shows that for $v_s < v_c$ the role of spin and charge wavepackets experience a

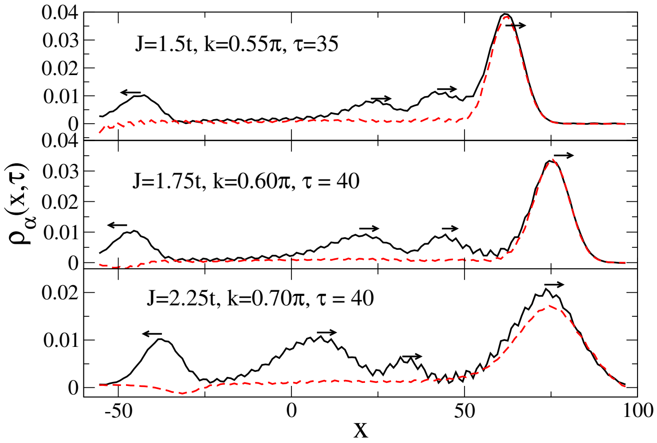

FIG. 5. (color online). Fractionalized wavepackets for different values of J/t away from the SUSY point, at a density $n = 0.6$. As in the SUSY case, charge fractionalizes into four pieces, while spin does not, and carries an appreciable amount of charge.

change with respect to fractionalization. In this case it is the spin density that splits into two fractions, one attached to the fastest fraction of charge, an another one left behind. Again, this new feature is not predicted by LL theory. However, no left propagating fraction of spin could be observed (excepting the depression due to finite-size effects). We therefore expect that this is due to SU(2) symmetry and the fact that in this case $K_s = 1$. As shown in Fig. 6, the amount of spin accompanying the charge increases as the momentum of the injected fermion increases. While such a phenomenon may suggest as in the lowest panel of Fig. 5 a total recombination of charge and spin as the energy increases, it is not total, since still a fraction of charge goes to the left, without accompanying spin.

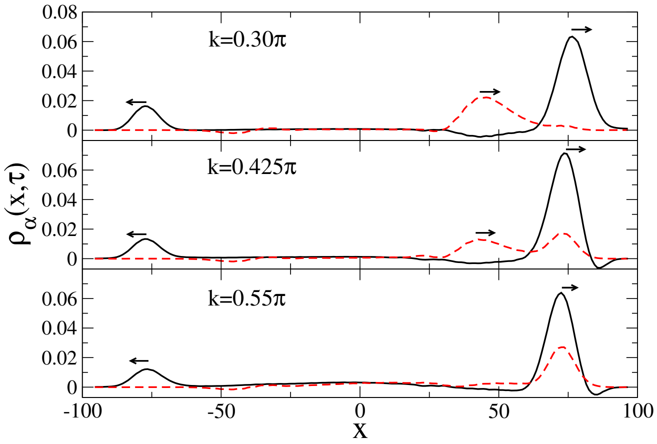

FIG. 6. (color online). Fractionalized wavepackets at $J/t = 1$, $n = 0.5$, $\tau = 50$ and $L = 200$. In this case, where $v_s < v_c$, fractionalization of the spin density is observed.

In summary, we have shown through the time evolution of an injected spinfull fermion onto the t-J model, that charge and spin fractionalization occurs beyond the predictions of the Luttinger liquid theory. A comparison with results from Bethe-Ansatz allowed to identify charge and spin excitations that split into components at high and low energies. The components at high energy reveal the dispersion ϵ_c and ϵ_s of charge and spin excitations, respectively. The components at low energy have a velocity that does not depend on the momentum of the injected fermion and are very well described by states at the pseudo-Fermi momenta of the charge excitation. This picture can be extended to a wide region in the phase diagram of the t-J model as long as the ground state corresponds to $K_c < 1$, and $v_s > v_c$. In this region fractionalization is observed only in the charge channel. However, for $v_c > v_s$, a region that develops for J/t below ~ 1.5, the spin density shows fractionalization. All over, the fastest excitation is accompanied by the complementary one, such that spin-charge separation is for them only partial. The other fractions present an almost complete spin-charge separation. Finally, we would like to remark, that the time evolution helped to visualize all the fractions in a more direct way than the study of the one-particle spectral function, where previous studies [28] only can identify the dispersion corresponding to fractions P_2 and P_4, but not those propagating at the pseudo-Fermi points.

A. M. and A. M. acknowledge support by the DFG through SFB/TRR 21. A. M. and J. M. P. C. thank the hospitality and support of the Beijing Computational Science Research Center, where part of the work was done. J. M. P. C. thanks the hospitality of the Institut für Theoretische Physik III, Universität Stuttgart, and the financial support by the Portuguese FCT under SFRH/BSAB/1177/2011, the German transregional collaborative research center SFB/TRR21, and Max Planck Institute for Solid State Research. A. M. thanks the KITP for hospitality. This research was supported in part by the National Science Foundation under Grant No. NSF PHY11-25915.

---

[1] V. V. Deshpande, M. Bockrath, L. Glazman, and A. Yacobi, Nature **464**, 209 (2010).
[2] T. Giamarchi, *Quantum Physics in One Dimension* (Clarendon Press, Oxford, 2004).
[3] T. Lorenz, M. Hofmann, M. Gruninger, A. Freimuth, G. S. Uhrig, M. Dumm, and M. Dressel, Nature **418**, 614 (2002).
[4] O. M. Auslaender, H. Steinberg, A. Yacoby, Y. Tserkovnyak, B. I. Halperin, K. W. Baldwin, L. N. Pfeiffer, and K. W. West, Science **308**, 88 (2005).
[5] C. Blumenstein, J. Schäfer, S. Mietke, A. Dollinger, M. Lochner, X. Y. Cui, L. Patthey, R. Matzdorf, and R. Claessen, Nature Phys. **7**, 776 (2011).
[6] K.-V. Pham, M. Gabay, and P. Lederer, Phys. Rev. B

61, 16397 (2000).

[7] H. Steinberg, G. Barak, A. Yacoby, L. N. Pfeiffer, K. W. West, B. I. Halperin, and K. L. Hur, Nature Phys. **4**, 116 (2008).

[8] A. Imambekov and L. I. Glazman, Science **323**, 228 (2009).

[9] A. Imambekov and L. I. Glazman, Phys. Rev. Lett **102**, 126405 (2009).

[10] T. L. Schmidt, A. Imambekov, and L. I. Glazman, Phys. Rev. Lett **104**, 116403 (2010).

[11] A. Shashi, L. I. Glazman, J.-S. Caux, and A. Imambekov, Phys. Rev. B **84**, 045408 (2011).

[12] J. M. P. Carmelo, K. Penc, and D. Bozi, Nucl. Phys. B **725**, 421 (2005); **737**, 351 (2006).

[13] G. Barak, H. Steinberg, L. N. Pfeiffer, K. W. West, L. Glazman, F. von Oppen, and A. Yacoby, Nature Phys. **6**, 489 (2010).

[14] S. R. White, Phys. Rev. Lett **69**, 2863 (1992).

[15] S. R. White, Phys. Rev. B **48**, 10345 (1993).

[16] S. R. White and A. E. Feiguin, Phys. Rev. Lett **93**, 076401 (2004).

[17] A. J. Daley, C. Kollath, U. Schollwöck, and G. Vidal, J. Stat. Mech.: Theor. Exp. P04005 (2004).

[18] U. Schollwöck, Rev. Mod. Phys. **77**, 259 (2005).

[19] U. Schollwöck, Ann. Phys. **326**, 96 (2011).

[20] P. A. Bares and G. Blatter, Phys. Rev. Lett **64**, 2567 (1990).

[21] P. A. Bares, G. Blatter, and M. Ogata, Phys. Rev. B **44**, 130 (1991).

[22] P. A. Bares, J. M. P. Carmelo, J. Ferrer, and P. Horsch, Phys. Rev. B **46**, 14624 (1992).

[23] M. Ogata, M. U. Luchini, S. Sorella, and F. F. Assaad, Phys. Rev. Lett **66**, 2388 (1991).

[24] A. Moreno, A. Muramatsu, and S. R. Manmana, Phys. Rev. B **83**, 205113 (2011).

[25] S. Söffing, I. Schneider, and S. Eggert, http://arxiv.org/abs/1204.0003 (2012).

[26] J. M. P. Carmelo, L. M. Martelo, and K. Penc, Nucl. Phys. B **737**, 237 (2006).

[27] For more details on the quantities extracted from Bethe-Ansatz, see the Supplementary Material.

[28] C. Lavalle, M. Arikawa, S. Capponi, F. F. Assaad, and A. Muramatsu, Phys. Rev. Lett **90**, 216401 (2003).